Cell. Mol. Life Sci. 65 (2008) 1256 – 1271
1420-682X/08/071256-16
DOI 10.1007/s00018-008-7587-3

Cellular and Molecular Life Sciences

Research Article

Coilin levels and modifications influence artificial reporter splicing

A. A. Whittom, H. Xu and M. D. Hebert*

Department of Biochemistry, The University of Mississippi Medical Center, 2500 North State Street, Jackson, MS 39216-4505 (USA), Fax: +1-601-984-1501, mhebert@biochem.umsmed.edu

Received 26 December 2007; received after revision 5 February 2008; accepted 7 February 2008
Online First 25 February 2008

Abstract. Cajal bodies (CBs) and Gems are nuclear domains that contain factors responsible for spliceosomal small nuclear ribonucleoprotein (snRNP) biogenesis. The marker protein for CBs is coilin. In addition to snRNPs, coilin and other factors, canonical CBs contain the survivor of motor neuron protein (SMN). SMN can also localize to Gems. Considering the important role that coilin plays in the formation and composition of CBs, we tested the splicing efficiency of several cell lines that vary in regards to coilin level and modification using an artificial reporter substrate. We found that cells with both hypomethylated coilin and Gems are more efficient at reporter splicing compared to cells in which SMN localizes to CBs. In contrast, coilin reduction, which induces Gem formation, decreases cell proliferation and artificial reporter splicing. These findings demonstrate that coilin modifications or levels impact artificial reporter splicing, possibly by influencing snRNP biogenesis.

Keywords. Coilin, SMN, Gems, Cajal body.

Introduction

The nucleus in eukaryotes is highly organized and contains numerous territories, domains and bodies [1–4]. Three such structures are promyelocytic leukemia (PML) bodies, Cajal bodies (CBs) and Gems (for Gemini of CBs). PML bodies are normally found in 10–20 nuclear foci and contain the PML protein plus numerous factors implicated in a variety of cellular functions such as transcriptional regulation [2, 5]. CBs and Gems contain factors that play a role in spliceosomal small nuclear ribonucleoprotein (snRNP) biogenesis. Notably, CBs and Gems contain the survival of motor neuron protein (SMN). Mutations in SMN result in spinal muscular atrophy (SMA), the leading genetic cause of childhood mortality [6]. In most cell lines (*e.g.*, HeLa cells from the American Type Culture Collection, HeLa-ATCC), nuclear SMN localizes in canonical CBs with the CB marker protein coilin, snRNPs and other factors. However, in a few cell lines (*e.g.*, HeLa-PV [7]), SMN is found in Gems. Gems also contain SMN-associated proteins known as Gemins, but lack snRNPs. No function for Gems has been described.

In addition to transformed cell lines, CBs and Gems can be found in normal tissues. Intriguingly, CB and Gem organization varies between cell type and developmental stage [8]. In the fetal spinal cord, for example, most nuclei contain both CBs and Gems. In contrast, adult spinal cord nuclei contain only CBs, and these CBs contain the proteins found in Gems. Other cell types, such as adult lung cells, lack CBs and Gems altogether. The fact that most cancer cell lines

* Corresponding author.

contain CBs, including those from the adult lung, indicates that the transformation process induces CB formation [9, 10]. Current evidence implicates the CB as the site for snRNP maturation [11], and active snRNP biogenesis is required for CB integrity [12–14]. The generation of U1, U2, U4 and U5 spliceosomal snRNPs, a complicated process, involves multiple maturation steps taking place in several different cellular compartments. During the cytoplasmic phase, SMN assists in the assembly of Sm proteins onto the snRNA components of snRNPs. After cap hypermethylation and 3′-end trimming, nascent snRNPs are imported into the nucleus, targeting first to the CB [15]. During this stage of snRNP biogenesis, the snRNA moiety is subject to modifications (2′-*O*-methylation and pseudouridylation) guided by small CB-specific RNAs (scaRNAs) [16–19]. Subsequently, newly generated snRNPs are stored in speckles.

Since snRNPs are vital for pre-mRNA processing, cells actively engaged in transcription (*e.g.*, neuronal and cancer cells) contain prominent CBs. The preponderance of CBs and Gems in fetal tissues may likewise reflect a high metabolic rate and increased need for splicing resources. Furthermore, the striking change in CB and Gem organization from fetal tissues (separate CBs and Gems) to adult tissues (CBs and Gems have fused into one structure, the canonical CB) strongly suggests that Gems may be needed in fetal tissues but not adult tissues. Presumably, the presence of Gem proteins such as SMN in CBs of adult tissues is sufficient to accommodate the unknown functions of Gems found in fetal cells. Again, however, the lack of CBs and Gems in some adult tissues clearly indicates that these structures are not invariant inhabitants of the nucleus, but rather reflect the overall RNP needs of the cell. In short, CBs and Gems can be thought of as efficiency platforms that facilitate activities that otherwise take place in the nucleoplasm. A recent study in fish has shown that coilin levels are increased and CBs are more prevalent in summer-acclimatized fish compared to those adapted to the cold season [20], reinforcing the fact that CB and Gem organization is dynamic and responsive to transcription and splicing demands of the cell.

With the exception of scaRNAs, all of the factors enriched in the CB also localize to other cellular compartments, such as the cytoplasm, nucleoplasm and nucleolus [2]. While only 30 % of coilin resides in this domain, the rest is nucleoplasmic [21]. The fact that almost all CB components can be found in other cell locales suggests that activities taking place within the CB also are likely to occur in the nucleoplasm. CB composition and nuclear dynamics suggest additional functions besides those centered upon snRNP maturation and maintenance. CBs are mobile, contain basal transcription factors and associate with snRNA genes (*e.g.*, U2 genes) and histone gene clusters, indicating an undefined role for the CB in RNA synthesis [22, 23]. CBs also associate with PML bodies [24, 25] and telomeres [26, 27]. Additionally, CBs contain telomerase RNA [28–30], indicating participation in the telomerase biogenesis and its delivery to telomeres.

The CB marker protein, coilin, may serve as the scaffold of CBs, bringing together various factors necessary for a range of functions into one nuclear subdomain, resulting in the most efficient platform to prepare these factors for their activities. In addition to the role coilin plays in CB association with PML bodies [25], coilin is recruited to centromeres in response to damage or depletion of CENP-B, indicating an undefined role in some type of centromere repair pathway [31]. Additionally, coilin post-translational modifications impact Gem formation. Coilin contains symmetrically dimethylated arginines that are important for direct interaction with SMN [32, 33] and the presence of Gems correlates with a decrease in coilin methylation [33, 34]. Coilin binds directly to several Sm proteins of snRNPs [32, 35], suggesting that direct coilin interaction with both SMN and snRNPs mediates their localization to CBs. Studies using cells lines with both CBs and Gems have shown that CBs involved in the nuclear phase of snRNP maturation are those containing SMN [36]. The interplay between coilin, SMN and snRNPs at the CB may therefore facilitate snRNP biogenesis and recycling. It is unknown if coilin in the nucleoplasm contributes to its putative role in the CB or possesses distinct nucleoplasmic-specific activities.

To better define the roles of coilin and CBs in the cell, mouse embryonic fibroblast (MEF) cell lines were derived from wild-type (WT) and coilin-knockout (KO) mice. Depending on their genetic backgrounds, some KO mice have significant viability and fertility problems, while others are phenotypically normal [37]. Cell lines derived from KO mice do not have canonical CBs but instead have two kinds of ′residual′ CBs [18, 37]. SMN does not accumulate in either kind of residual CB found in KO cells, underscoring the role of coilin in the formation of canonical CBs [18, 37]. In HeLa cells depleted of coilin by RNA interference (RNAi), CBs are abolished, Gem formation is induced and proliferation is reduced compared to control treated cells [12]. In contrast, work on *Arabidopsis* has identified a coilin ortholog (Atcoilin) that, in addition to other loci, impacts CB formation and size [38]. However, no obvious growth phenotype in *Arabidopsis* mutants lacking CBs was detected. Coilin, therefore, is not an essential protein and, by extension, the CB is not required for survival. Rather, it appears that coilin and CBs ensure that cells can

efficiently adapt to changing splicing requirements. This ability may account for the conservation of coilin and CBs from plants to animals.

Notwithstanding the clear role that coilin plays in CB formation, other data demonstrate that coilin alone does not determine overall CB formation, composition and function. *Drosophila*, for example, have CBs but lack a detectable coilin ortholog [39]. Additionally, transient expression of SmB (a component of snRNPs), but not coilin, induces CB formation in cells that normally lack this structure [36]. Knockdown of SMN by RNAi [12–14] or inhibition of snRNP biogenesis using leptomycin B [40] disrupts CBs. Moreover, the modification of endogenous snRNA still takes place in MEF KO cells with residual CBs [18]. Thus, it is likely that residual CBs are capable of performing functions attributed to canonical CBs. It is not known, however, if cells lacking canonical CBs and coilin are less efficient in these activities.

To examine the efficiency by which cells with variable coilin levels and CB and Gem organization generate functional snRNPs, different cell lines were challenged with an artificial splicing substrate. Cells containing both hypomethylated coilin and Gems (HeLa-PV) were more efficient at reporter splicing compared to cells with canonical CBs (HeLa-ATCC). In contrast, cells with reduced coilin levels were found to have impaired splicing and cell proliferation rates compared to WT lines. These findings are consistent with the proposed role of CBs in the efficient formation of splicing machinery, and also provide correlative data suggesting that the presence of Gems in fetal tissues may facilitate snRNP activity.

Materials and methods

Cell lines and cell culture. HeLa-PV and MEF cell lines were obtained from Dr. Greg Matera (Case Western Reserve University, Cleveland, OH). HeLa strain ATCC was obtained from the American Type Culture Collection (Manassas, VA). HeLa-tTS cells were purchased from BD Biosciences (San Jose, CA). Cells were cultured as previously described [25] except HeLa-tTS cells were cultured with Tet-System approved FBS (Clontech, Mountain View, CA) with 100 μg/ml G418 (Invitrogen, Carlsbad, CA) used for maintenance. For stable selection, HeLa-tTS cells were subjected to 200 μg/ml hygromycin B (Invitrogen) and 100 μg/ml hygromycin B was utilized for maintenance. Where indicated, doxycycline (Clontech) was added to culture medium at a final concentration of 0.125 μg/ml. Cells transfected with pSI were harvested 24 h following transfection. Actinomycin D (Sigma-Aldrich, St. Louis, MO) was used at 5 μg/ml for 6 h.

Antibodies, immunofluorescence and Western blotting. Immunofluorescence and Western blotting was performed as previously described [25]. Briefly, slides were fixed for immunofluorescence using 4.0 % paraformaldehyde for 10 min, followed by a rinse in 1× PBS and then a 5-min incubation in 0.5 % Triton X-100. After this incubation, the slides were washed three times in 1× PBS for 5 min at room temperature. For staining, slides were incubated with blocking solution followed by incubations with the appropriate primary and secondary antibodies and washing steps. Coilin monoclonal antibody Pδ was purchased from Abcam (Cambridge, MA) or Sigma-Aldrich. Coilin polyclonal antibody H-300 was purchased from Santa Cruz Biotechnology (Santa Cruz, CA). SMN monoclonal antibody was from BD Biosciences and β-tubulin was from Dr. Sharon Lobert (University of Mississippi Medical Center, Jackson, MS). For Western blotting, cells were lysed in 50 μl high salt nuclear lysis buffer (50 mM Tris, pH 7.5, 0.5 M NaCl, 2 mM EDTA, 1 % sodium deoxycholate, 1 % NP-40, 0.1 % SDS), followed by addition of 150 μl no-salt lysis buffer, then briefly sonicated.

DNA constructs. The pSI vector was purchased from Promega (Madison, WI). The Knockout Inducible RNAi System H with RNAi-Ready pSiren-RetroQ-TetH, a tetracycline-responsive expression vector, was purchased from Clontech. The pCR2.1 vector was purchased from Invitrogen.

Mammalian cell transfection, generation of stable cell lines and RNAi. Short interfering RNAs (siRNAs), purchased from Dharmacon (Lafayette, CO), include the non-targeting control (catalog no. D-001210–01–20), human coilin smart pool reagent (M-019894–00–0020) and four separate coilin siRNAs. HeLa-ATCC cells were transiently transfected with 100 nM control or coilin pool siRNA, or one of four different coilin siRNAs for 48 h. Transfections using siRNA were performed according to the Lipofectamine 2000 siRNA transfection protocol (Invitrogen). The two most potent siRNA sequences were used to design shRNA oligonucleotides that were generated (Integrated DNA Technologies, Coralville, IA), annealed and ligated into the RNAi-Ready pSiren-RetroQ-TetH vector. To generate stable cell lines expressing shRNAs, vectors were stably integrated into HeLa-tTS cells containing the tetracycline-controlled transcriptional silencer (tTS). In theory, addition of tetracycline (or doxycycline) to HeLa-tTS media should cause tTS dissociation from the shRNA promoter region, resulting in shRNA expression then processing into siRNA. To ensure that transformation, selection and doxycycline addition do not

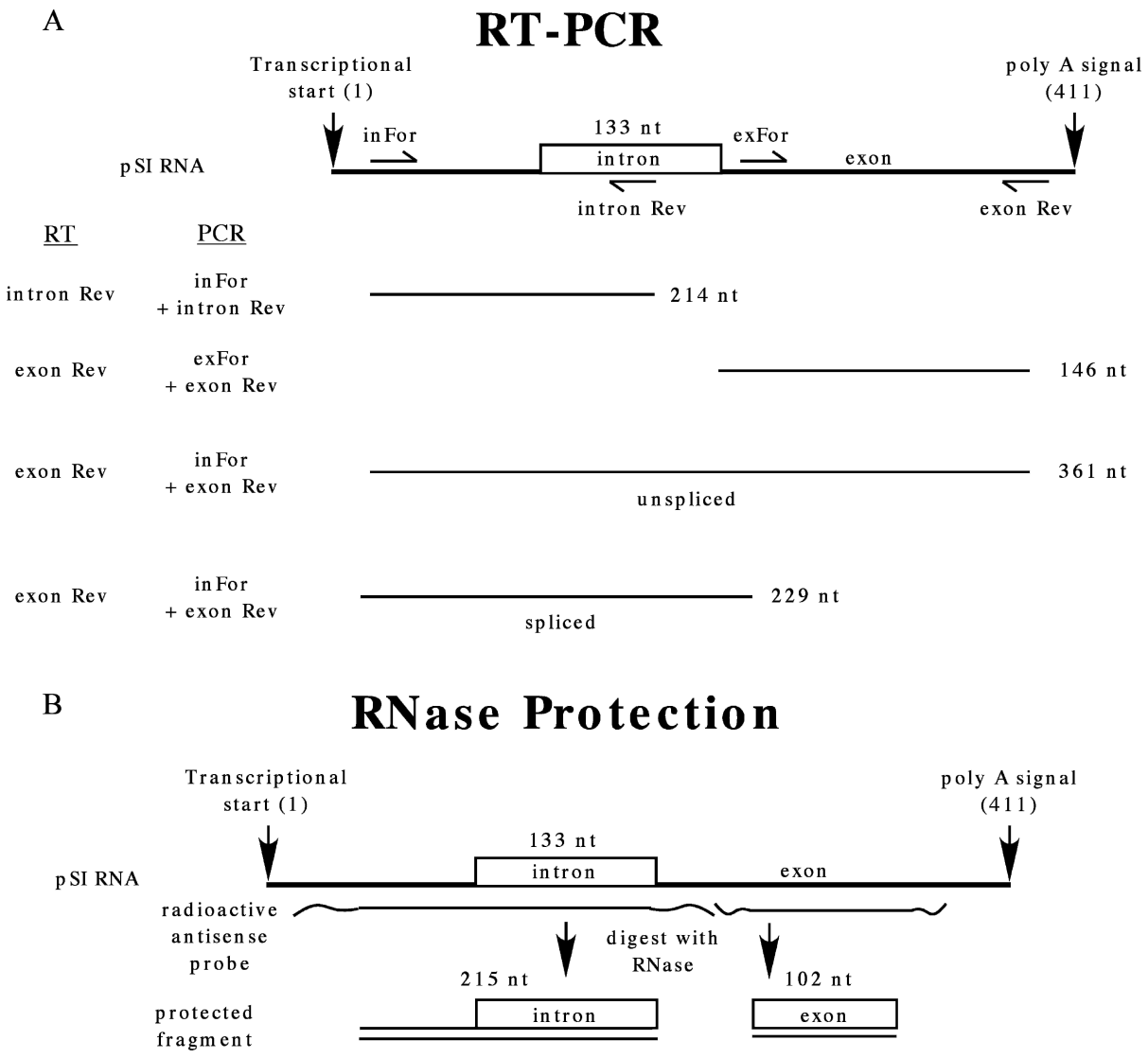

Figure 1. An artificial substrate to challenge the splicing machinery. (*A*) For RT-PCR or qRT-PCR, RNA isolated from cells transfected with pSI is subjected to an RT-PCR reaction using indicated primers to separately amplify intron and exon fragments. An alternative approach for RT-PCR is amplification of both unspliced and spliced message in the same reaction. The locations of primers used and expected sizes of the products are shown. For RNase protection assays (*B*), RNA, isolated from cells transfected with pSI, is hybridized with complementary radiolabeled antisense probes. The sizes of the protected fragments are shown.

alter CB and Gem organization or coilin levels, a control shRNA oligonucleotide (not targeting any RNA) was cloned into the vector and used for stable integration. For stable integration, the Pantropic Retroviral Expression System (Clontech) with the GP2–293 packaging cell line was utilized according to the manufacturer's directions. Viral infection medium was added to HeLa-tTS cells, followed by stable cell selection using 100 μg/ml G418 and 200 μg/ml hygromycin B. Stable cell colonies were picked and then maintained in 100 μg/ml G418 and 100 μg/ml hygromycin B.

Primers. The primers for reverse transcriptase (RT)-PCR, qRT-PCR and the cloning of templates used to generate antisense RNA probes (Fig. 1) are shown in Table 1.

Transfection of pSI and RNA isolation. HeLa-ATCC, HeLa-PV and HeLa-tTS shRNA stable cells were transfected for 18 h using Superfect (Qiagen, Valencia, CA). Cells were harvested followed by RNA isolation using the RNAqueous RNA isolation kit (Ambion, Austin, TX). The resultant RNAs were DNase treated with Turbo DNase (Ambion) according to the manufacturer's instructions. Where indicated, cells were grown for 2 days in the presence of

Table 1. Primers used.

1	5′-AGGCTTTTGCAAAAAGCTTGATTCTTCTGACACAACAG-3′	pSI intron For
2	5′-GTGTCCACTCCCAGTTCAATTACAGCTCTTAAG-3′	pSI-exon For
3	5′-ATTTAGGTGACACTATAGANNNNNNCTGTGGAGAGAAAGGCAAAG-3′	pSI intron antisense containing Sp6 promoter
4	5′-ATTTAGGTGACACTATAGANNNNNNGGGTCGACTCTAGAGGTACCACGC-3′	pSI exon antisense containing Sp6 promoter
5	5′-GTGGAGAGAAAGGCAAAGTGG-3′	pSI intron Rev
6	5′-CTCATCAATGTATCTTATCATGTCTGCTCGAAGCG-3′	pSI exon Rev
7	5′-GTACTTCAGGGTGAGGATGCCTCTCTTG-3′	Human β-actin Rev
8	5′-GGGCCGTCTTCCCCTCCATCGTGG-3′	Human β-actin For
9	5′-GTCTTGGGTCAATCAACTCTTTCC-3′	Human coilin Rev
10	5′-CTTGAGAGAACCTGGGAAATTTG-3′	Human coilin For
11	5′-CTGTGCTGTGGAAGCTAAGTCCTG-3′	Human β-actin For intron
12	5′-CAGGTCAGCTCAGGCAGGAAAGAC-3′	Human β-actin Rev intron

doxycycline, followed by transfection with pSI and incubation for an additional 18 h in medium containing doxycycline.

RT-PCR. RNA isolated from pSI-transfected cells was subjected to RT-PCR utilizing the AccessQuick RT-PCR System (Promega). Either primers 1 and 5 or primers 2 and 6 were utilized for both reverse transcription and PCR amplification in a one-step reaction. To avoid non-linear amplification at high cycle numbers, low cycle numbers of 23 cycles or less were used. Combined use of primers 1 and 5 results in amplification of a 214-nucleotide (nt) fragment of the pSI intron. Combined use of primers 2 and 6 results in amplification of a 146-nt fragment of the pSI exon (Fig. 1A). The RT-PCR samples were run on a 2% agarose gel, stained with ethidium bromide, and the band intensities quantified. The values obtained were used to calculate the ratio of intron to exon for each set of bands, and the average of the value sets was normalized. RNA was also utilized in a one-step RT-PCR reaction using primers 1 and 6, resulting in the amplification of both spliced and unspliced message in the same reaction. The unspliced message results in a 361-nt band, while the spliced message, lacking the intron, results in a 229-nt band (Fig. 1A). The RT-PCR samples were run on a 2% agarose gel, stained with ethidium bromide, and the band intensities quantified. The values obtained were used to calculate the ratio of unspliced to spliced message for each set of bands and the average of the value sets was normalized. Reactions lacking RT were performed for all samples.

RNase protection assays. RNase protection assays (RPA) were conducted as described in the RPA III kit from Ambion. Antisense probes to pSI RNA fragments were made from linearized DNA templates containing Sp6 promoters. The template for the pSI-intron was amplified using primers 1 and 3; the template for the pSI-exon was amplified using primers 2 and 4. These amplified fragments were cloned into pCR2.1. Before conducting the transcription reaction using the Sp6 MAXIscript kit (Ambion), templates were linearized with *Xho*I (pSI-intron) or *Hind*III (pSI-exon) restriction enzymes (New England Biolabs, Ipswich, MA). Probes were generated as described in the MAXIscript kit protocol. Protected probes were resolved on an 8% polyacrylamide gel followed by autoradiography and quantification.

Quantitative real-time RT-PCR. Reaction mixtures (25 μl) containing RNA isolated from pSI-transfected cells and the same primer sets utilized in RT-PCR to separately amplify pSI intron or exon, were utilized for quantitative real-time RT-PCR (qRT-PCR). Primers 9 and 10 were used to detect coilin. β-actin exon was detected with primers 7 and 8, while β-actin intron was detected using primers 11 and 12. Reactions lacking RT were performed for all samples. The rates of pSI intron or exon amplification, Ct values, and dissociation curve analyses confirming the specificity of resulting products were determined using the Brilliant SYBR Green II qRT-PCR Master Mix kit (Stratagene, La Jolla, CA), and the MX3000P and MX3005P Real-Time PCR Systems (Stratagene) according to the manufacturer's instructions. The values obtained were used to quantify data using the $2^{(-\Delta\Delta CT)}$ method [41] to compare relative expression.

Cell proliferation assays. C48, 5C6 and C4–5 cells were counted using a Coulter counter and seeded into three sets of T25 s containing medium with or without doxycycline. After 24 h, one set of T25 s was harvested and the cells were counted. This was repeated at 48

and 72 h after seeding. Proliferation rates were determined by dividing the cell number obtained at day 3 by that obtained at seeding. These values were then normalized to that obtained for C48 cells grown in the absence of doxycycline.

Image processing and quantification. Image acquisition for immunofluorescence and Western blotting was performed as previously described [25]. For all RT-PCR studies, gel images were captured with a Kodak DC290 digital camera. Western blot chemiluminescent signals captured by X-ray film and band intensities from RT-PCR gel images were quantified using NIH Image 1.63 software (a public domain program developed at the U.S. National Institutes of Health for the Macintosh computer, http://rsb.info.nih.gov/nih-image/). Adobe Photoshop 7.0 (San Jose, CA) and Canvas 8 (Deneba Systems, Miami, FL) were used for image labeling and processing

Statistical data analysis. Significant differences for data obtained from RT-PCR, qRT-PCR, RPA analysis and cell proliferation assays were determined using Student's *t*-test (a *p* value of less than 0.05 is considered significant). Histogram error bars represent percent error about the mean.

Results

The hypothesis that governs our work is that cells with canonical CBs are able to generate snRNPs more efficiently, and therefore have a greater splicing potential, compared to cells without CBs. To test this hypothesis, we decided to challenge the splicing resources of cells having variable coilin levels and CB and Gem organization using an artificial splice substrate. The pSI plasmid was chosen as this substrate because it contains a chimeric intron composed of the 5′-donor site from the first intron of the human β-globin gene and the 3′-acceptor site from an immunoglobulin gene intron [42]. The sequences of the donor, acceptor and branchpoint sites were modified by the manufacturer to match the consensus sequences for splicing [43]. The transcript is under the control of the SV40 promoter. To compare the splicing efficiencies of the pSI artificial substrate among the different cell lines, RT-PCR, qRT-PCR and RPA were utilized (Fig. 1).

HeLa-PV cells exhibit increased pre-mRNA splicing efficiency compared to HeLa-ATCC cells. HeLa-ATCC cells have canonical CBs containing both coilin and SMN, whereas, in HeLa-PV cells, SMN can localize to CBs and Gems [2, 7]. To assess if cells with Gems are more or less efficient in pre-mRNA splicing compared to cells with canonical CBs, we challenged HeLa-ATCC and HeLa-PV cells with the pSI reporter plasmid. RT-PCR was performed to separately amplify pSI intron and exon. Although HeLa-ATCC and HeLa-PV have comparable exon signals (Fig. 2A, lanes 3 and 5), the intron signal in HeLa-ATCC cells is significantly greater than that found in HeLa-PV cells (Fig. 2A, compare lanes 2 and 4). Upon quantification and comparison of the pSI intron/exon ratio in HeLa-ATCC and HeLa-PV cells, we observed that HeLa-PV cells were approximately 27 % more efficient in splicing the pSI transcript (p=1.0282E-05, histogram). To verify these results, RT-PCR was performed to amplify both spliced and unspliced pSI transcripts in a single reaction. More unspliced product is detected in RNA isolated from HeLa-ATCC compared to that found in HeLa-PV cells (Fig. 2B, compare upper intron bands in lanes 2 and 4 to those in lanes 3 and 5). By quantifying the ratio of unspliced to spliced message, we found that, by this method, HeLa-PV cells are approximately 37 % more efficient in splicing the pSI transcript compared to HeLa-ATCC (p=0.001, histogram). By these methods, HeLa-PV cells are approximately 30–40 % more efficient at splicing the pSI message compared to HeLa-ATCC cells. Reactions lacking RT, performed for all samples, did not yield products.

Next, RPAs were conducted and similar exon signals for both HeLa-ATCC and HeLa-PV cells were detected (Fig. 2C, compare lanes 2 and 6). In contrast, the HeLa-ATCC intron signal is stronger compared to that for HeLa-PV (compare lanes 1 and 5). Upon comparing the intron to exon ratios, HeLa-PV cells are approximately 70 % more efficient at splicing the pSI message compared to HeLa-ATCC cells (p=0.00027, histogram). The larger disparity between splicing efficiency observed using RPA compared to the two RT-PCR methods most likely reflects the fact that RPA is the more quantifiable technique. RT-PCR and RPA experiments were conducted from eight independently obtained RNA samples for each cell line (normalized to HeLa-ATCC). The differences observed between HeLa-ATCC and HeLa-PV do not appear to be the result of variation in overall coilin amounts considering that both lines have approximately the same relative coilin message levels (our unpublished results). In summary, the methods used here show that HeLa-PV, which contains hypomethylated coilin, non-canonical CBs and Gems, is more efficient at splicing the pSI artificial reporter compared to HeLa-ATCC cells, which have canonical CBs.

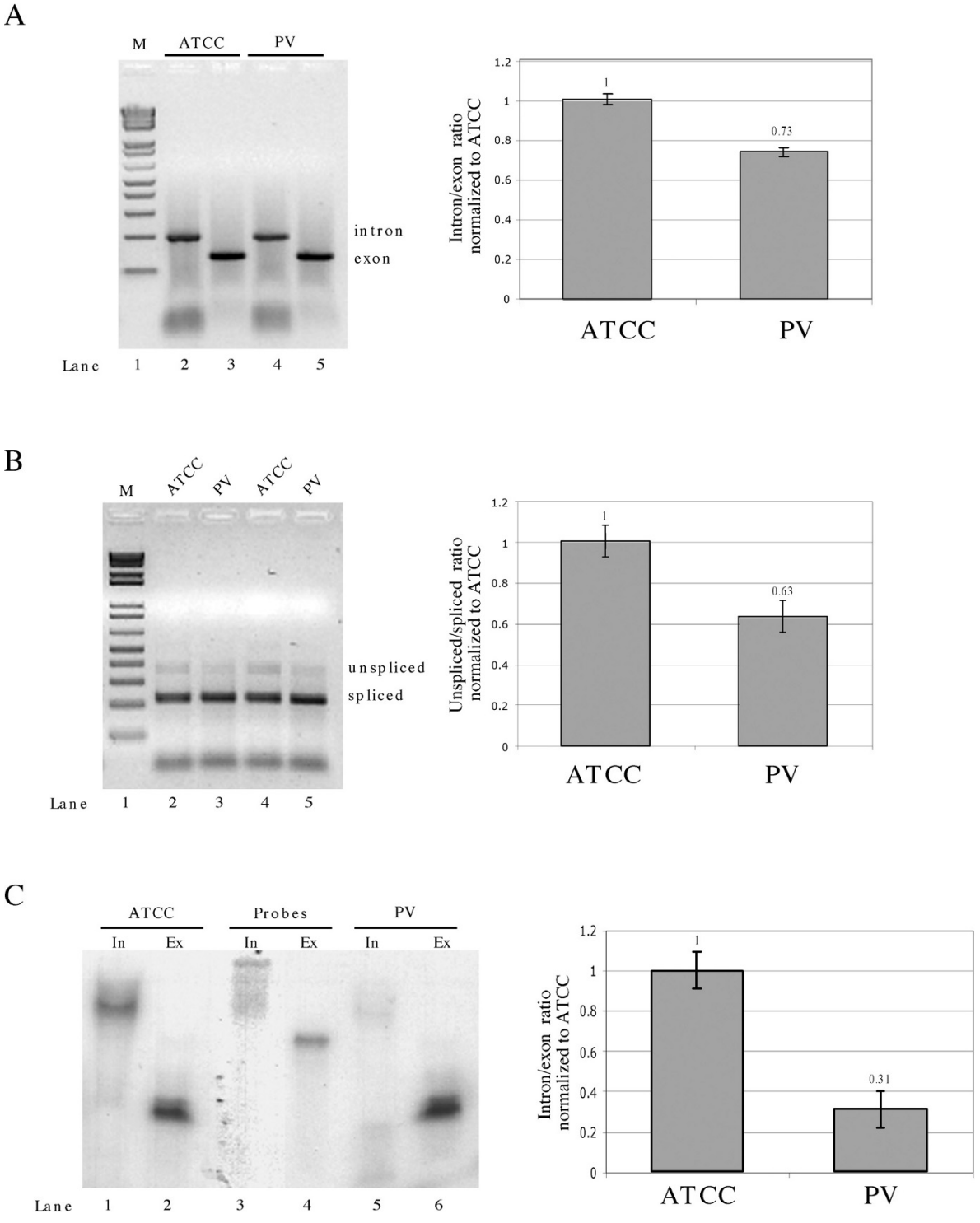

Figure 2. HeLa-PV cells are more efficient in splicing the pSI message than HeLa-ATCC cells. (*A*) RNA isolated from HeLa-PV and HeLa-ATCC cells transfected with pSI was subjected to RT-PCR to amplify pSI message containing intronic (lanes 2 and 4) or exonic (lanes 3 and 5) fragments from both HeLa-ATCC and HeLa-PV RNA. The intron/exon ratio in HeLa-PV is significantly different than that found in HeLa-ATCC (p=1.0282E-5). (*B*) RT-PCR was used to amplify pSI message containing both spliced and unspliced pSI sequences in the same reaction from both HeLa-ATCC (lanes 2 and 4) and HeLa-PV (lanes 3 and 5) RNA. The intron/exon ratio in HeLa-PV is significantly different than that found in HeLa-ATCC (p=0.001). (*C*) RNase protection assays using intronic or exonic antisense probes hybridized to the pSI message isolated from both HeLa-ATCC and HeLa-PV transfected cells. Similar exon signals for both HeLa-ATCC (lane 2) and HeLa-PV cells (lane 6) were detected, yet significantly more intron signal was detected for HeLa-ATCC cells (lane 1) compared to HeLa-PV (lane 5). The intron/exon ratio in HeLa-PV is significantly different than that found in HeLa-ATCC (p=0.00027). Each experiment was conducted using eight independently obtained RNAs for each cell line. Histograms depict averaged results for each set of experiments.

Coilin KO MEF cells do not efficiently splice the pSI reporter message. MEF cell lines derived from WT and coilin-KO mice [37] provide an excellent cell biological resource that can be used to test the role of coilin and the CB as an efficiency factor. More specifically, studies comparing similarly generated WT and KO cells have the potential to elucidate how the absence of coilin and CBs affects splicing activities. MEF KO cells do not have canonical CBs containing SMN and snRNPs, but instead have two kinds of residual CBs: one that contains nucleolar proteins such as fibrillarin and another that contains scaRNAs [18, 37]. Although KO cells have been shown to properly modify snRNAs [18], no studies have challenged these cells with a substrate that could be used to monitor the efficiency of splicing.

To monitor the splicing capacity of MEF WT and KO cells, RNA isolated from cells transiently transfected with the pSI plasmid was subjected to RPA conducted from three independently obtained RNA samples for each cell line (normalized to WT) (Fig. 3). The pSI intron signals are about the same in WT and KO (compare lanes 2 and 3). However, KO exon signals are significantly lower compared to WT (compare lanes 4 and 5). Although WT and KO have comparable intron signals, the intron/exon ratio for KO cells is increased by 86 % compared to WT (p=0.0036). Low cycle PCR amplification of DNA extracted from the transfected cells verified that approximately equal amounts of the pSI vector were transfected into the different cell lines (our unpublished results). Strikingly, therefore, despite the fact that both WT and KO cells received equal levels of the pSI plasmid, the steady-state level of the pSI message is significantly reduced by more than sixfold in the KO background. Since this message is reduced and the intron signal relative to the exon signal is greatly elevated in KO compared to WT, KO cells are not only deficient in their ability to splice the pSI message, but may also have additional defects associated with transcription. This transcription deficit was observed for other reporters and endogenous transcripts as assessed by bromouridine (BrU) pulse labeling (our unpublished observations). Similar to the reduced proliferation rate found in HeLa cells following knockdown of coilin by RNAi [12], we have found that KO cells take substantially longer to double compared to WT cells (WT, 26 h doubling time; KO, 53 h doubling time). Taken together, these findings suggest that coilin reduction impacts both splicing and, unexpectedly, transcription rates, leading to longer doubling times.

Knockdown of coilin by RNAi disrupts CBs and induces Gem formation. To better understand how the lack of coilin affects CB and Gem organization and

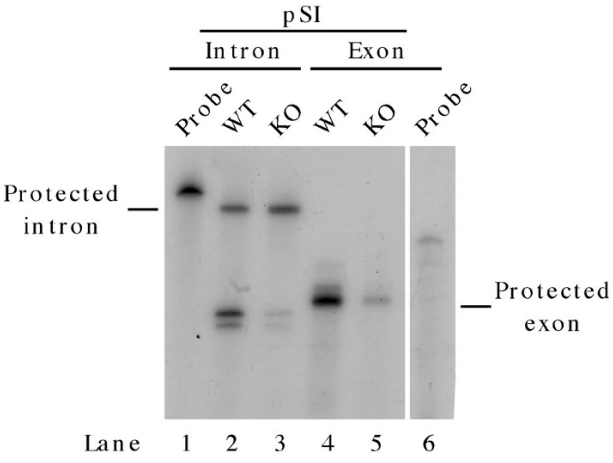

Figure 3. Mouse embryonic fibroblast (MEF) knockout (KO) cells do not efficiently splice the pSI message as compared to wild-type (WT) cells. MEF WT and KO cells were challenged with the pSI plasmid and RNase protection assays were conducted. The pSI intron signals similar for WT (lane 2) and KO (lane 3), while the KO exon signal (lane 5) is significantly lower compared to WT (lane 4). The intron/exon ratio for KO is significantly different than that found in WT (p=0.0036). Experiments were conducted using three independently obtained RNAs for each cell line.

splicing, we knocked down coilin in HeLa-ATCC cells by transient transfection with coilin pool siRNA. HeLa-ATCC cells normally have canonical CBs with coilin, SMN and snRNPs. Control siRNA does not affect CB structure, as verified by coilin and SMN staining (Fig. 4A, top row, arrows). In contrast, coilin siRNA abolishes CBs, but SMN foci (Gems) are still present (Fig. 4A, bottom row, arrows). Another group has reported identical results [12]. Western blotting demonstrates that coilin levels are reduced in the presence of coilin siRNA, but not control siRNA, while SMN protein levels are unaffected (Fig. 4B). Since coilin reduction in HeLa cells has been shown to reduce cell proliferation and alter CB and Gem organization [12], we next explored if splicing would likewise be impaired.

Generation and characterization of stable coilin RNAi cell lines. To study the role of CBs and Gems in pre-mRNA splicing in the most genetically similar background possible, we generated stable coilin RNAi cell lines. We utilized control shRNA (clone C48) and coilin shRNA (clones 5C6 and C4–5) cell lines. Comparison of coilin levels relative to β-tubulin by Western blotting reveals that coilin in the 5C6 cell line is reduced by 70 % compared to that found in the control C48 cell line (Fig. 5A). This coilin reduction was observed in the absence of doxycycline, and did not change upon the addition of this drug. Thus, within the limits of detection at the protein level, the expression of the coilin shRNA and subsequent knockdown of coilin in the 5C6 cell line is leaky and

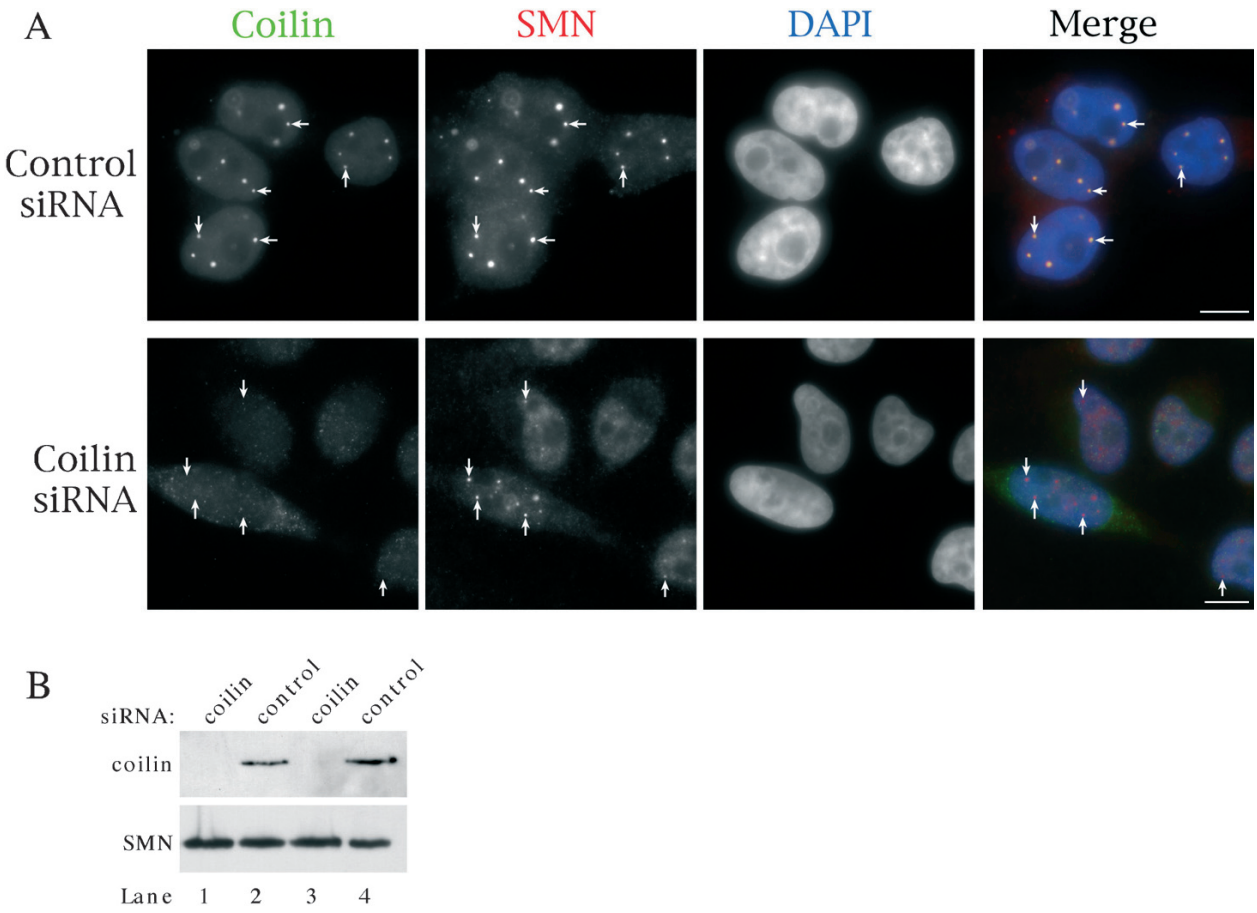

Figure 4. Coilin siRNA treatment disrupts canonical Cajal bodies (CBs), induces gem formation and results in the reduction of coilin expression. (*A*) HeLa-ATCC cells transiently transfected with control or coilin siRNA were fixed and subjected to coilin and SMN antibody staining. Canonical CBs, containing coilin and SMN, can be observed in cells treated with control siRNA (top panels, arrows). In contrast, cells treated with coilin siRNA lack CBs but have gems (bottom panels, arrows). Scale bar, 10 μm. (*B*) Western blot of HeLa-ATCC extract treated with coilin or control siRNA. Coilin (top panel) and SMN (bottom panel) were detected. Note that the coilin signal is essentially absent in coilin siRNA treated extract (lanes 1 and 3), but SMN levels are comparable to that found in control extract.

not doxycycline responsive. Transient expression of coilin siRNAs has been shown to reduce cell proliferation rates in HeLa cells by approximately 50% [12]. Also, in agreement with the report using transiently transfected coilin siRNAs [12], we find that the 5C6 proliferation rate is reduced by approximately 40% ($p = 8.68\text{E-}6$), while C4–5 proliferates at approximately 80% the rate of C48 ($p = 0.0031$) (Fig. 5B). Proliferation rates were not significantly affected in any cell line by the addition of doxycycline. While Western blotting demonstrated only a sight reduction in C4–5 coilin levels relative to β-tubulin compared to C48 (our unpublished results), proliferation rates were slowed in C4–5 compared to C48. To determine the extent of coilin reduction in 5C6 and C4–5 compared to C48, we conducted qRT-PCR to amplify coilin and β-actin from three independently obtained RNA samples for each cell line (grown with or without doxycycline for 2 days). In the absence of doxycycline, both 5C6 and C4–5 were found to have reduced relative coilin message levels to only 60% the level of C48 in 5C6 ($p=0.0038$) and 75% the level of C48 in C4–5 ($p=0.037$) (Fig. 5C). Curiously, it was observed that doxycycline increases relative coilin levels in C48 and C4–5 (Fig. 5C). The possibility that coilin levels in C48 remain the same in the presence of doxycycline while β-actin levels are decreased is not supported: C48 coilin levels are also increased by doxycycline when compared to the GAPDH housekeeping message, while the ratio of β-actin to GAPDH does not change (our unpublished results). This strongly suggests that doxycycline impacts coilin levels, complicating our analysis into its effect on inducing coilin shRNA synthesis in 5C6 and C4–5. However, 5C6 coilin levels do not increase in the presence of doxycycline, possibly due to increased coilin shRNA production. Despite these complications, in the absence of doxycycline, both 5C6 and C4–5 have reduced relative coilin message levels and impaired cell proliferation rates (Fig. 5B) compared

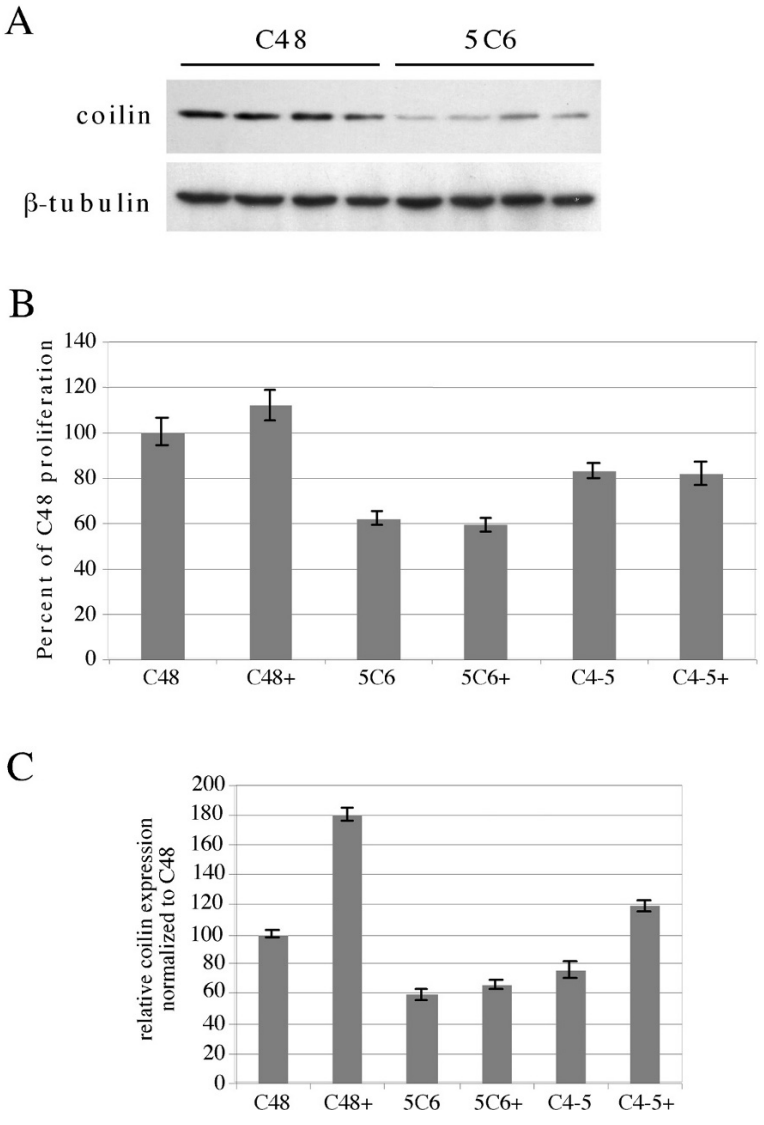

Figure 5. Reduction of coilin expression in a stable cell line expressing coilin shRNA results in a decreased cell proliferation rate. (*A*) Western blot of control-shRNA (C48) and coilin-shRNA (5C6) extract from cells grown in the absence of doxycycline. Coilin levels relative to β-tubulin reveal that 5C6 has a 70% reduction in coilin compared to C48. (*B*) Proliferation rates of stable shRNA cell lines. 5C6 and C4–5 lines have reduced proliferation rates compared to C48 ($p = 8.68E\text{-}6$ and 0.0031, respectively). Treatment with doxycycline (+) does not significantly change proliferation rates. (*C*) QRT-PCR analysis of coilin expression relative to β-actin using three independently obtained RNAs for each cell line grown with or without doxycycline. 5C6 and C4–5 have reduced coilin message levels compared to C48 ($p = 0.0038$ and 0.037, respectively).

to C48. These lines should thus be suitable to test our hypothesis that cells with higher coilin levels and canonical CBs have a greater splicing potential compared to cells with lower coilin levels and disrupted CBs or lacking this structure altogether.

Next, we examined if coilin reduction in the 5C6 and C4–5 cell lines disrupts CBs and induces Gem formation as observed in cells transiently transfected with coilin siRNA (Fig. 4) [12]. Immunofluorescence staining with antibodies to coilin and SMN reveals clear differences between the number of CBs and Gems found in C48 *versus* 5C6 or C4–5 cells grown in the absence of doxycycline (Fig. 6). In particular, 21% of interphase 5C6 cells lacked CBs, compared to 7% of C48 cells (Fig. 6, row B; Table 2). Since CBs disassemble in mitosis and reform in early G1 [44], it is normal for a fraction of cells not to have visible CBs. In 5C6, however, the number of cells without CBs is far more than expected and observed compared to C48. We also observed that 5C6 cells more frequently contain Gems (38%) compared to C48 cells (8%) (Fig. 6, row C; Table 2). 5C6 cells that did have canonical CBs had, on average, significantly fewer per cell (2.3) than that found in the C48 cell line (4.3) (Fig. 6, rows A and D; Table 2). In C4–5 cells, the number of canonical CBs per cell (3.8) is more similar to that found in C48 cells (Table 2). Interestingly, nucleolar cap-like structures, reminiscent of those observed when transcription is inhibited [45], were observed in the C4–5 line in approximately 20% of cells (Fig. 6, row E). These cap-like structures were uncommon in C48 or 5C6 cells. Therefore, reduced levels of coilin in the 5C6 and C4–5 cell lines correlate with alterations in the organization of CBs and Gems. These findings, coupled with the cell proliferation data, suggest that normal snRNP biogenesis and

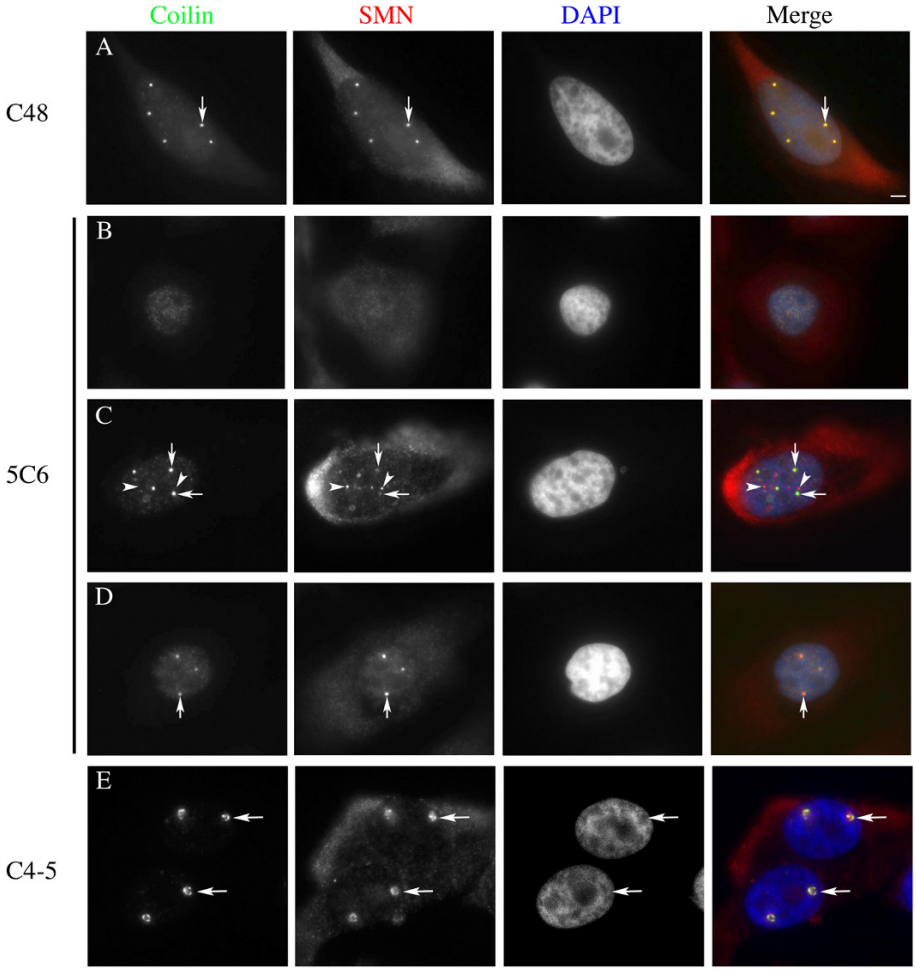

Figure 6. Coilin reduction in the 5C6 and C4–5 cell lines disrupts CB and Gem organization. Immunofluorescence staining was conducted on the C48, 5C6 and C4-5 cell lines for coilin (green) and SMN (red) with DAPI staining (blue) to detect the nucleus. The merged image of all three channels is shown in the right column. Row A, typical control C48 cell with canonical CBs containing coilin and SMN (one of which is marked by an arrow). Rows B–D, predominant phenotypes of the 5C6 cell line: (B) no CBs or Gems; (C) CBs and Gems. Some CBs are marked with arrows, Gems with arrowheads. (D) Canonical CBs containing coilin and SMN. Row E, nucleolar cap-like structures observed in approximately 20% of C4–5 cells (arrows). Scale bar, 2 μm.

activity may be perturbed in the 5C6 and C4–5 cell lines.

Splicing efficiency of stable coilin shRNA subclones and control shRNA cell lines. To ascertain if the reduced coilin levels, impaired cell proliferation rates and CB and Gem reorganization observed in the 5C6 and C4–5 cell lines correspond to changes in splicing efficiency, we challenged C48, 5C6 and C4–5 lines cultured without doxycycline by transient transfection with the pSI plasmid. RNA isolated from these lines was subjected to a single RT-PCR reaction (for C48 and 5C6 only) to amplify spliced and unspliced pSI message in the same reaction, or qRT-PCR to separately amplify pSI intron or exon (all three lines). RT-PCR reactions lacking RT, performed for all samples, did not yield products. RT-PCR and qRT-PCR experiments were conducted from three independently obtained RNA samples each for C48 and 5C6 (normalized to C48). As shown in Figure 7 using RT-PCR, comparison of the ratio of unspliced (upper bands) to spliced (lower bands) signals from C48 and 5C6 cells, we found that 5C6 cells contain approximately 1.6-fold more unspliced message (p=0.0001, histogram). Corroborating these results, qRT-PCR experiments revealed that the relative level of intronic pSI message was increased by approximately 3-fold in 5C6 (p=1.49E-5) and 4-fold in C4–5 (p=6.3E-7), upon normalization to the level found in C48 (Fig. 8A).

Our data showing that pSI splicing in 5C6 and C4–5 is impaired compared to C48 clearly indicates a connection between disrupted CB organization and splicing efficiency. Although these results are consistent with alterations in pre-mRNA splicing, possibly as a consequence of disrupted snRNP biogenesis, they could conceivably be the result of increased mRNA stability factors, or a diminished capacity of the 5C6 and C4–5 cell lines to degrade mRNA. To address this possibility, qRT-PCR for pSI intron or exon was performed on two independently obtained RNA samples from C48 and 5C6 cells incubated with actinomycin D, a transcription inhibitor. After transcription inhibition, the level of unspliced message in 5C6 (normalized to C48) was actually lower than that found in the control C48 line (p=0.0324) (Fig. 8B).

Table 2. Analysis of Cajal body (CB) and Gem composition in stable shRNA cell lines.

Cell line[a]	Expressed shRNA	Canonical CBs per cell[b,c]	% cells with only canonical CBs[b,c]	% cells with Gems[d]	% cells lacking CBs and Gems[d]	% cells other structures[e]
C48	Control	4.3±0.22[f]	78	8	7	7
5C6	Coilin	2.3±0.24[f]	31	38	21	10
C4-5	Coilin	3.8±0.28[g]	52	19	5	24

[a] A minimum of 100 cells, cultured without doxycycline, was characterized for each cell line.
[b] Based on an average number of canonical CBs (having both coilin and SMN) per cell for each cell line.
[c] Excludes cells categories having Gems, lacking CBs and Gems or other structures.
[d] Based on the total number of cells counted for each cell line.
[e] Excludes cells categories having Gems, lacking CBs and Gems and only canonical CBs.
[f] Compared to C48 ($p = 9.46E-07$).
[g] Compared to C48 ($p = 0.017$).

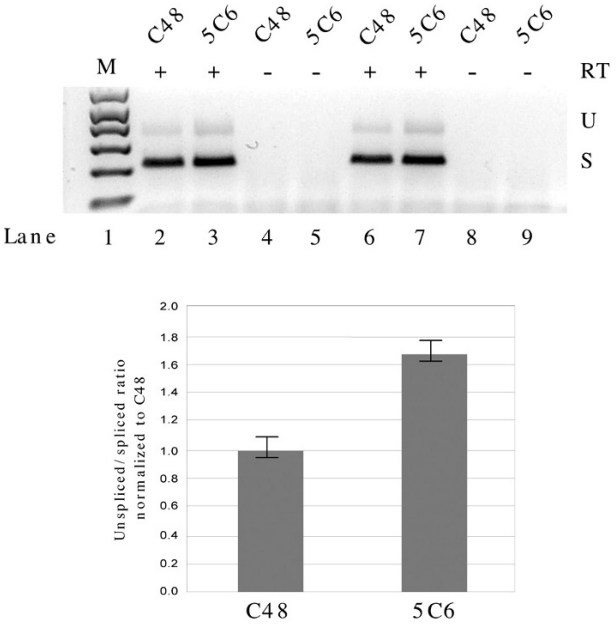

Figure 7. Stable coilin shRNA-expressing cells (5C6) are less efficient in splicing the pSI message compared to control shRNA-expressing cells (C48). RT-PCR was used in one reaction to amplify both spliced (lower bands, S) and unspliced (upper bands, U) pSI fragments. Additional reactions were done in the absence of reverse transcriptase as a negative control demonstrating that DNA contamination was not present (lanes 4, 5, 8 and 9). The values obtained were used to calculate the ratio of unspliced to spliced message for each separate experiment, normalized to the C48 value and the results were averaged (histogram). For example, in C48 lane 2, the value for the upper, unspliced product is 311, while the lower spliced product value is 4530. This yields a ratio of unspliced to spliced of 0.0687. In 5C6 lane 3, the value for the unspliced band is 526, while the spliced band is 5190, yielding a ratio of 0.101. These ratios are then normalized to the C48 ratio, yielding a 1.47-fold increase (0.101/0.0687 = 1.47) in the amount of unspliced product found in 5C6 compared to C48. C48 cells were found to be more efficient in splicing the pSI transcript compared to 5C6 cells ($p = 0.0001$). Data for histogram derived from experiments using at least three different RNA samples for each cell line. Error bars represent percent error about the mean.

These findings indicate that mRNA may in fact be less stable in 5C6 compared to that found in C48, strengthening our belief that impaired splicing is the cause for the increased levels of unspliced message observed in 5C6 (Figs. 7, 8A).

Finally, we examined if we could detect an increase in the frequency of unspliced endogenous message in the coilin knockdown 5C6 and C4–5 lines. Two independently obtained RNA samples each for C48, 5C6 and C4–5 cells were subjected to qRT-PCR for both spliced and unspliced β-actin message. As shown in Fig. 8C, we did not detect an increase in the relative level of unspliced β-actin message in the 5C6 and C4–5 lines compared to C48. In fact, 5C6 has an apparent decrease in the relative amount of unspliced actin compared to C48. Although this reduction was not statistically significant, it may be a reflection of the decreased mRNA stability present in 5C6 as determined by the use of actinomycin D (Fig. 8B). In summary, the stable reduction of coilin in the 5C6 and C4–5 cell lines disrupts CBs, induces Gem formation, impairs cell proliferation and perturbs artificial reporter splicing.

Discussion

In this study, we provide evidence that different coilin levels and variable CB and Gem organization can impact artificial reporter splicing efficiencies. Since its description by Santiago Ramon-y-Cajal in 1903, modest headway has been made towards understanding the actual function(s) of the enigmatic subnuclear domain that now bears his name. For example, it has been shown that snRNAs of snRNPs are modified in the CB [18], confirming that CBs participate in snRNP biogenesis. However, any possible function ascribed to the CB has to be reconciled with the reality that many cell types (*e.g.*, adult lung tissue) do not have CBs [8, 9]. Thus, the activities that take place within the CB likely can also occur in the nucleoplasm. Why then has the CB been conserved throughout evolution? What advantage does this subnuclear domain confer? The current thinking with regards to

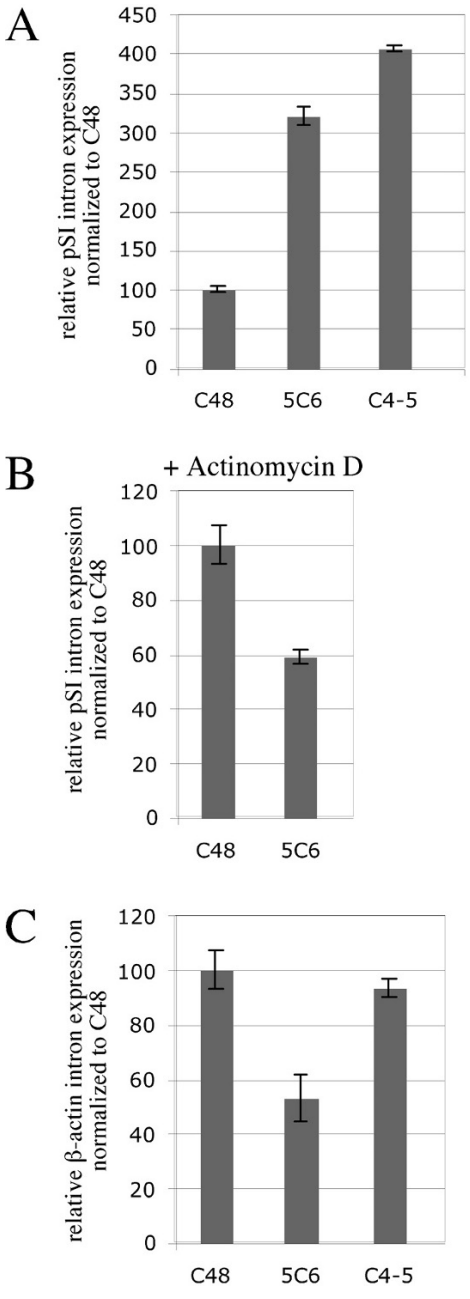

Figure 8. qRT-PCR analysis of splicing in control (C48) and coilin knockdown (5C6, C4–5) cell lines. (*A*) RNA from pSI-transfected cells was subjected to qRT-PCR to separately amplify pSI intron and exon. The intron to exon ratio in 5C6 and C4–5 is significantly different than that found in C48 (p=1.49E-5 and 6.3E-7, respectively). Experiments were conducted using three independently obtained RNAs for each cell line. (*B*) Actinomycin D treatment of pSI transfected C48 and 5C6 cell lines. Isolated RNA from actinomycin D-treated cells was subjected to qRT-PCR to amplify pSI intron and exon. Experiments were conducted using two independently obtained RNAs for each cell line grown without doxycycline. 5C6 was found to have approximately 40% less intron compared to C48 ($p = 0.0324$). (*C*) Analysis of endogenous mRNA splicing. Amplification of β-actin intron and exon by qRT-PCR demonstrates that 5C6 has an apparent 40% decrease in the relative amount of intron compared to C48, but this difference is not statistically significant. Experiments were conducted using two independently obtained RNAs for each cell line grown without doxycycline.

RNA processing is that the CB is an efficiency platform that facilitates snRNP biogenesis, snRNP regeneration and Sm protein reclamation [11, 22, 35, 46, 47]. Recent work examining the trafficking of newly imported and steady-state snRNPs in living cells provides further evidence for these CB functions [48].

In sharp contrast to the known activities and potential cellular benefits of CBs, the rationale for fetal tissues having Gems remains perplexing. If canonical CBs containing, among other factors, coilin, snRNPs and SMN reflect the most efficient platform for RNP-generating functions in adult cells, then it is possible that the combination of CBs and Gems in fetal cells may likewise reflect their optimal configuration. In other words, the observed developmental diversity of CBs and Gems in fetal and adult tissues [8] may be indicative of a hierarchy of CB and Gem organization with regard to snRNP generation. By this logic, rapidly dividing fetal cells containing CBs and Gems would represent the most efficient snRNP generation platform, followed by adult cells with canonical CBs. Cells lacking CBs (*e.g.*, adult lung cells) would be expected to have the least capacity to generate functional snRNPs.

To test this model, we challenged a variety of cells with an artificial splice substrate reporter. The cell lines used can be classified into three types: (i) cells most resembling fetal tissues containing non-canonical CBs and Gems (HeLa-PV), (ii) cells resembling adult tissues containing canonical CBs (HeLa-ATCC, C48, MEF WT), and (iii) cells with reduced coilin levels and Gem induction (MEF KO, 5C6, C4–5). Although HeLa-PV, MEF KO, 5C6 and C4–5 cells have Gems, it is important to appreciate that the mechanism(s) by which these lines came to have Gems differs. In HeLa-PV, coilin is not properly modified by symmetrical dimethylation, possibly leading to perturbed SMN retention in the CB and subsequent formation of Gems [33, 34]. In contrast, MEF KO, 5C6 and C4–5 cells have Gems because of decreased coilin levels [37] (Figs. 5 and 6, Table 2). Therefore, it was expected that MEF KO, 5C6 and C4–5 lines would have problems with some aspects of the CB snRNP-generating pathway and consequently have reduced splicing potential. This was observed (Figs. 3, 7 and 8). Additionally, MEF KO, 5C6 and C4–5 lines have reduced cell proliferation rates compared to control lines, consistent with the results obtained when HeLa cells are transiently transfected with coilin siRNA [12]. However, MEF WT and KO results should be interpreted cautiously since differences in the transformation process may exist between these lines that could account for observed differences in pSI splicing unrelated to CB and Gem organization. Additionally,

MEF KO cells may not truly be devoid of coilin; they have the potential to make the coilin N-terminal self-association domain [37, 49]. It is not known what effect (if any) this fragment may have on RNA synthesis and processing activities. Although MEF KO cells displayed phenotypes consistent with what would be expected for cells lacking coilin and functional CBs (*i.e.*, impaired splicing and proliferation rates), and HeLa-PV cells (having Gems) presented with greater splicing potential, to more conclusively assess if different coilin modifications or levels impact splicing, we performed additional experiments using other cell lines.

Unlike the MEF KO line [37], immunofluorescence analysis of the 5C6 line demonstrates that the remaining coilin is sufficient to form canonical CBs, albeit fewer of them, in a subset of cells. Other cells, however, contain CBs and Gems or lack both of these structures (Fig. 6, Table 2). Interestingly, the C4–5 line displays nucleolar cap-like structures in a subset of cells similar to that observed when normal (*e.g.*, HeLa-ATCC) cells are treated with the transcription inhibitor actinomycin D (Fig. 6, Table 2). It should be pointed out that this interesting phenotype is, for some reason, detectable in only 20% of the C4–5 cells. Consequently, a generalized effect on transcription through the entire cell cycle is hard to explain. Since all lines are transfected with the same amount of pSI plasmid, an easy indicator of transcriptional efficiency is to compare the ratio of the pSI exon message to a housekeeping message. We have observed that the ratio of the pSI exon message relative to a housekeeping message (β-actin or GAPDH) is approximately the same in the C4–5 line as it is in the C48 and 5C6 lines. If the C4–5 line indeed had problems with transcription (as found in coilin KO MEFs), then we would expect that this ratio would be different in this line compared to the other two. It is possible, therefore, that this line is altered differently by reduced coilin levels compared to 5C6, in which these structures are uncommon. Likewise, the pSI exon/housekeeping message ratio can also be used to demonstrate that, given the same amount of pSI plasmid and expression level, differences are observed in the level of unspliced message present between the C48, 5C6 and C4–5 lines. If there is an effect of expression level on splicing, then this effect has been controlled for. Consequently, we believe that it is not the expression level of the plasmid that affects its splicing, but rather its cellular context.

In line with the current understanding of coilin function, it is clear from the studies presented here that overall coilin levels influence CB and Gem formation in transformed cell lines. These changes may alter the ability of the 5C6 or C4–5 lines to generate functional snRNPs, leading to the observed reduction in artificial reporter splicing efficiency (Figs. 7 and 8A). In addition to the artificial reporter construct used here, we have also investigated the splicing of an endogenous transcript, β-actin, in the 5C6, C4–5 and C48 cell lines. We could not detect an increase in unspliced β-actin message in the coilin-KO cell lines compared to that found in the C48 line (Fig. 8C). This is not an entirely unexpected result, but may simply reflect the fact that, since transcription and splicing occur concurrently in ′mRNA factories′ or ′transcriptosomes′ [22, 50], an endogenous transcript may not be made if it cannot be properly spliced. The observed impaired proliferation rates of 5C6 and C4–5 may thus be the result of an overall reduction in the number of transcriptosomes due to inefficient snRNP biogenesis. As opposed to endogenous transcripts, the artificial splice reporter used here is under the control of a viral promoter, and therefore may generate sufficient numbers of transcripts such that deficiencies in splicing can be detected.

Another interesting finding of our studies is that cells with hypomethylated coilin, non-canonical CBs and Gems (HeLa-PV) are more efficient in artificial reporter splicing compared to cells with canonical CBs (HeLa-ATCC) (Fig. 2). Although these results are correlative, they support our belief that cells with both CBs and Gems (*e.g.*, fetal cells) represent the CB and Gem organization with the highest potential for snRNP generation. Future experiments are being designed to more directly assess the role of coilin methylation in contributing to CB and Gem organization and snRNP biogenesis. For example, it would be ideal if we could generate a cell line that, upon addition of a drug, simultaneously abolishes WT coilin and induces a coilin mutant that cannot be dimethylated. Such a cell line would closely approximate the CB and Gem organization of fetal tissue, providing a single genetic background that should help clarify the role of CBs and Gems in snRNP biogenesis.

The data we present here provide a link between splicing capacity, coilin levels and CB and Gem organization. In particular, we show that cells in which coilin is reduced by stable shRNA expression are impaired in both artificial reporter splicing and cell proliferation. Elegant studies by Carmo-Fonseca and colleagues [51] showed that cells in which CBs have been disrupted by anti-coilin antibody injection are capable of splicing both adenoviral and human β-globin transcripts when challenged 24 h after CB disappearance. Given the long half-lives of spliceosomal snRNPs (20 h, [52]), it is possible that the time course of these experiments did not allow the level of pre-existing snRNPs to drop enough to detect alterations in splicing. The use of a stable coilin shRNA cell

line resolves this dilemma. Our current work centers upon the clarification as to exactly why 5C6 and C4–5 cells display a reduction in artificial reporter splicing. To resolve this issue, we are planning on challenging these lines with an snRNA substrate. Since the CB is a known site of snRNA modification by 2′-*O*-methylation and pseudouridylation [16, 18], inefficiencies in the ability of the knockdown lines to modify this substrate relative to the control C48 cell line would be consistent with altered CB function.

Acknowledgements. We thank Dr. G. Matera (Case Western Reserve University, Cleveland, OH) for the MEF and HeLa-PV cell lines. We also thank Dr. S. Negi for assistance with development of stable shRNA cell lines and A. Alise Reiken for assistance with immunofluorescence slide preparation. This work was supported by a grant from the Muscular Dystrophy Association.

1 Lamond, A. I. and Earnshaw, W. C. (1998) Structure and function in the nucleus. Science 280, 547–553.
2 Matera, A. G. (1999) Nuclear bodies: Multifaceted subdomains of the interchromatin space. Trends Cell Biol. 9, 302–309.
3 Spector, D. L. (2001) Nuclear domains. J. Cell Sci. 114, 2891–2893.
4 Zimber, A., Nguyen, Q. D. and Gespach, C. (2004) Nuclear bodies and compartments: Functional roles and cellular signalling in health and disease. Cell. Signal. 16, 1085–1104.
5 Maul, G. G., Negorev, D., Bell, P. and Ishov, A. M. (2000) Review: Properties and assembly mechanisms of ND10, PML bodies, or PODs. J. Struct. Biol. 129, 278–287.
6 Frugier, T., Nicole, S., Cifuentes-Diaz, C. and Melki, J. (2002) The molecular bases of spinal muscular atrophy. Curr. Opin. Genet. Dev. 12, 294–298.
7 Liu, Q. and Dreyfuss, G. (1996) A novel nuclear structure containing the survival of motor neurons protein. EMBO J. 15, 3555–3565.
8 Young, P. J., Le, T. T., Dunckley, M., Nguyen, T. M., Burghes, A. H. and Morris, G. E. (2001) Nuclear gems and Cajal (coiled) bodies in fetal tissues: Nucleolar distribution of the spinal muscular atrophy protein, SMN. Exp. Cell Res. 265, 252–261.
9 Spector, D. L., Lark, G. and Huang, S. (1992) Differences in snRNP localization between transformed and nontransformed cells. Mol. Biol. Cell 3, 555–569.
10 Young, P. J., Le, T. T., thi Man, N., Burghes, A. H. and Morris, G. E. (2000) The relationship between SMN, the spinal muscular atrophy protein, and nuclear coiled bodies in differentiated tissues and cultured cells. Exp. Cell Res. 256, 365–374.
11 Matera, A. G. and Shpargel, K. B. (2006) Pumping RNA: Nuclear bodybuilding along the RNP pipeline. Curr. Opin. Cell Biol. 18, 317–324.
12 Lemm, I., Girard, C., Kuhn, A. N., Watkins, N. J., Schneider, M., Bordonne, R. and Luhrmann, R. (2006) Ongoing U snRNP biogenesis is required for the integrity of Cajal bodies. Mol. Biol. Cell 17, 3221–3231.
13 Girard, C., Neel, H., Bertrand, E. and Bordonne, R. (2006) Depletion of SMN by RNA interference in HeLa cells induces defects in Cajal body formation. Nucleic Acids Res. 34, 2925–2932.
14 Shpargel, K. B. and Matera, A. G. (2005) Gemin proteins are required for efficient assembly of Sm-class ribonucleoproteins. Proc. Natl. Acad. Sci. USA 102, 17372–17377.
15 Sleeman, J. E. and Lamond, A. I. (1999) Newly assembled snRNPs associate with coiled bodies before speckles, suggesting a nuclear snRNP maturation pathway. Curr. Biol. 9, 1065–1074.
16 Darzacq, X., Jady, B. E., Verheggen, C., Kiss, A. M., Bertrand, E. and Kiss, T. (2002) Cajal body-specific small nuclear RNAs: A novel class of 2′-O-methylation and pseudouridylation guide RNAs. EMBO J. 21, 2746–2756.
17 Jady, B. E. and Kiss, T. (2001) A small nucleolar guide RNA functions both in 2′-O-ribose methylation and pseudouridylation of the U5 spliceosomal RNA. EMBO J. 20, 541–551.
18 Jady, B. E., Darzacq, X., Tucker, K. E., Matera, A. G., Bertrand, E. and Kiss, T. (2003) Modification of Sm small nuclear RNAs occurs in the nucleoplasmic Cajal body following import from the cytoplasm. EMBO J. 22, 1878–1888.
19 Kiss, A. M., Jady, B. E., Darzacq, X., Verheggen, C., Bertrand, E. and Kiss, T. (2002) A Cajal body-specific pseudouridylation guide RNA is composed of two box H/ACA snoRNA-like domains. Nucleic Acids Res. 30, 4643–4649.
20 Alvarez, M., Nardocci, G., Thiry, M., Alvarez, R., Reyes, M., Molina, A. and Vera, M. I. (2007) The nuclear phenotypic plasticity observed in fish during rRNA regulation entails Cajal bodies dynamics. Biochem. Biophys. Res. Commun. 360, 40–45.
21 Lam, Y. W., Lyon, C. E. and Lamond, A. I. (2002) Large-scale isolation of Cajal bodies from HeLa cells. Mol. Biol. Cell 13, 2461–2473.
22 Gall, J. G. (2000). Cajal bodies: The first 100 years. Annu. Rev. Cell Dev. Biol. 16, 273–300.
23 Ogg, S. C. and Lamond, A. I. (2002) Cajal bodies and coilin – Moving towards function. J. Cell Biol. 159, 17–21.
24 Grande, M. A., van der Kraan, I., van Steensel, B., Schul, W., de The, H., van der Voort, H. T., de Jong, L. and van Driel, R. (1996) PML-containing nuclear bodies: Their spatial distribution in relation to other nuclear components. J. Cell Biochem. 63, 280–291.
25 Sun, J., Xu, H., Subramony, S. H. and Hebert, M. D. (2005). Interactions between Coilin and PIASy partially link Cajal bodies to PML bodies. J. Cell Sci. 118, 4995–5003.
26 Jady, B. E., Richard, P., Bertrand, E. and Kiss, T. (2006) Cell cycle-dependent recruitment of telomerase RNA and Cajal bodies to human telomeres. Mol. Biol. Cell 17, 944–954.
27 Tomlinson, R. L., Ziegler, T. D., Supakorndej, T., Terns, R. M. and Terns, M. P. (2006) Cell cycle-regulated trafficking of human telomerase to telomeres. Mol. Biol. Cell 17, 955–965.
28 Lukowiak, A. A., Narayanan, A., Li, Z. H., Terns, R. M. and Terns, M. P. (2001) The snoRNA domain of vertebrate telomerase RNA functions to localize the RNA within the nucleus. RNA 7, 1833–1844.
29 Zhu, Y., Tomlinson, R. L., Lukowiak, A. A., Terns, R. M. and Terns, M. P. (2004) Telomerase RNA accumulates in Cajal bodies in human cancer cells. Mol. Biol. Cell 15, 81–90.
30 Jady, B. E., Bertrand, E. and Kiss, T. (2004) Human telomerase RNA and box H/ACA scaRNAs share a common Cajal body-specific localization signal. J. Cell Biol. 164, 647–652.
31 Morency, E., Sabra, M., Catez, F., Texier, P. and Lomonte, P. (2007) A novel cell response triggered by interphase centromere structural instability. J. Cell Biol. 177, 757–768.
32 Hebert, M. D., Szymczyk, P. W., Shpargel, K. B. and Matera, A. G. (2001) Coilin forms the bridge between Cajal bodies and SMN, the spinal muscular atrophy protein. Genes Dev. 15, 2720–2729.
33 Hebert, M. D., Shpargel, K. B., Ospina, J. K., Tucker, K. E. and Matera, A. G. (2002) Coilin methylation regulates nuclear body formation. Dev. Cell 3, 329–337.
34 Boisvert, F. M., Cote, J., Boulanger, M. C., Cleroux, P., Bachand, F., Autexier, C. and Richard, S. (2002) Symmetrical dimethylarginine methylation is required for the localization of SMN in Cajal bodies and pre-mRNA splicing. J. Cell Biol. 159, 957–969.
35 Xu, H., Pillai, R. S., Azzouz, T. N., Shpargel, K. B., Kambach, C., Hebert, M. D., Schumperli, D. and Matera, A. G. (2005) The C-terminal domain of coilin interacts with Sm proteins and U snRNPs. Chromosoma 114, 155–166.
36 Sleeman, J. E., Ajuh, P. and Lamond, A. I. (2001) snRNP protein expression enhances the formation of Cajal bodies containing p80-coilin and SMN. J. Cell Sci. 114, 4407–4419.

37 Tucker, K. E. Berciano, M., Jacobs, E., LePage, D., Shpargel, K., Rossire, J., Chan, E., Lafarga, M., Conlon, R. and Matera, A. G. (2001) Residual Cajal bodies in coilin knockout mice fail to recruit Sm snRNPs and SMN, the spinal muscular atrophy gene product. J. Cell Biol. 154, 293–307.
38 Collier, S., Pendle, A., Boudonck, K., van Rij, T., Dolan, L. and Shaw, P. (2006) A distant coilin homologue is required for the formation of Cajal bodies in *Arabidopsis*. Mol. Biol. Cell 17, 2942–2951.
39 Liu, J. L., Murphy, C., Buszczak, M., Clatterbuck, S., Goodman, R. and Gall, J. G. (2006) The *Drosophila melanogaster* Cajal body. J. Cell Biol. 172, 875–884.
40 Carvalho, T., Almeida, F., Calapez, A., Lafarga, M., Berciano, M. T. and Carmo-Fonseca, M. (1999) The spinal muscular atrophy disease gene product, SMN: A link between snRNP biogenesis and the Cajal (coiled) body. J. Cell Biol. 147, 715–728.
41 Livak, K. J. and Schmittgen, T. D. (2001) Analysis of relative gene expression data using real-time quantitative PCR and the $2(^{-\Delta\Delta}CT)$ method. Methods 25, 402–408.
42 Bothwell, A. L., Paskind, M., Reth, M., Imanishi-Kari, T., Rajewsky, K. and Baltimore, D. (1981) Heavy chain variable region contribution to the NPb family of antibodies: Somatic mutation evident in a gamma 2a variable region. Cell 24, 625–637.
43 Senapathy, P., Shapiro, M. B. and Harris, N. L. (1990) Splice junctions, branch point sites, and exons: Sequence statistics, identification, and applications to genome project. Methods Enzymol 183, 252–278.
44 Carmo-Fonseca, M., Ferreira, J. and Lamond, A. I. (1993) Assembly of snRNP-containing coiled bodies is regulated in interphase and mitosis – Evidence that the coiled body is a kinetic nuclear structure. J. Cell Biol. 120, 841–852.
45 Carmo-Fonseca, M., Pepperkok, R., Carvalho, M. T. and Lamond, A. I. (1992) Transcription-dependent colocalization of the U1, U2, U4/U6 and U5 snRNPs in coiled bodies. J. Cell Biol. 117, 1–14.
46 Schaffert, N., Hossbach, M., Heintzmann, R., Achsel, T. and Luhrmann, R. (2004) RNAi knockdown of hPrp31 leads to an accumulation of U4/U6 di-snRNPs in Cajal bodies. EMBO J. 23, 3000–3009.
47 Stanek, D., Rader, S. D., Klingauf, M. and Neugebauer, K. M. (2003) Targeting of U4/U6 small nuclear RNP assembly factor SART3/p110 to Cajal bodies. J. Cell Biol. 160, 505–516.
48 Sleeman, J. (2007) A regulatory role for CRM1 in the multidirectional trafficking of splicing snRNPs in the mammalian nucleus. J. Cell Sci. 120, 1540–1550.
49 Hebert, M. D. and Matera, A. G. (2000) Self-association of coilin reveals a common theme in nuclear body localization. Mol. Biol. Cell 11, 4159–4171.
50 Bentley, D. (2002) The mRNA assembly line: Transcription and processing machines in the same factory. Curr. Opin. Cell Biol. 14, 336–342.
51 Almeida, F., Saffrich, R., Ansorge, W. and Carmo-Fonseca, M. (1998) Microinjection of anti-coilin antibodies affects the structure of coiled bodies. J. Cell Biol. 142, 899–912.
52 Moore, M. J., C. C. Query, and P. Sharp (1993) The RNA World. Cold Spring Harbor Laboratory Press, Cold Spring Harbor.